



# A detailed numerical study of the evolution of soot particle size distributions in laminar premixed flames

Jörg Appel<sup>a</sup>, Henning Bockhorn<sup>a,\*</sup>, Michael Wulkow<sup>b</sup>

<sup>a</sup> *Institut für Chemische Technik & Engler Bunte Institut – Bereich Verbrennungstechnik, Universität Karlsruhe (TH), Kaiserstraße 12, 76128 Karlsruhe, Germany*

<sup>b</sup> *Computing in Technology GmbH (CiT), Oldenburger Straße 200, 26180 Rastede, Germany*

## Abstract

In this work, two numerical techniques, viz. the method of moments and a discrete h-p-Galerkin method, have been applied for numerical simulation of soot formation in a laminar premixed acetylene/oxygen/argon flame. From the evolution of the PAH and the soot particle size distributions, new insight into the different processes of soot formation is provided. For this, the single submodels have been examined with respect to their influence on the PAH and the soot particle size distributions. The particle inception step was studied in detail by comparing the simulated PAH size distributions with experimental results. Additionally, an estimation of the interaction energy of layered PAH dimers was performed by quantum chemical calculations. From these results, some evidence for the particle inception model employing coalescence of PAH molecules has been found. The numerical results for the gas phase chemical species, the particle number densities and volume fractions of soot as well as for the soot particle size distributions are compared with experimental data. Thereby, the consistency of the entire model is demonstrated. © 2001 Elsevier Science Ltd. All rights reserved.

*Keywords:* PAHs; PAHs size distribution; Soot formation; Particle size distributions; Numerical simulation

## 1. Introduction

The formation of products of incomplete combustion is a persistent problem in combustion research. To obtain a fundamental insight into the complex physical and chemical phenomena during pollutant formation in flames, a detailed study of the underlying processes is necessary. For the formation of soot, the efforts at developing detailed kinetic models have been intensified in recent years (see Kennedy, 1997). The quality of predictions has approached a quantitative level.

From the perspective of numerical simulation, a detailed model of soot formation and oxidation has to treat the gas phase and solid phase separately and, finally, has to give information about the interaction be-

tween them. For laminar premixed flames, which are the subject of the present work, the governing conservation equations for the energy and the species mass fractions are formulated as one-dimensional in physical space. These equations can be solved numerically for a relatively large number of chemical species and no further simplifications are necessary to obtain the detailed flame structure. Chemical mechanisms describing the main combustion reactions are relatively reliable, whereas the kinetics of the formation of large linear aliphatic and polycyclic aromatic hydrocarbons are under lively discussion (Leung and Lindstedt, 1995; Marinov et al., 1996; Wang and Frenklach, 1997). The prediction of soot particle size distributions depends on the capability of the underlying kinetic model to predict concentration profiles of soot precursors and of reactive radicals.

The numerical treatment of the dynamics of the solid phase, viz. the soot particle ensemble, is in general more

\* Corresponding author.

complicated. The balance equations of the particle number densities for different soot particle sizes result in a system of equations, the size of which is prohibitive to their solution with standard numerical techniques.

To overcome this problem, Frenklach and Harris (1987) introduced the method of moments, where the soot particle size distribution is represented by its statistical moments. The method has the advantage, that the computational effort to obtain useful information such as the total particle number density  $N$  and soot volume fraction  $F_V$  is relatively low. Relations among higher order moments, for example, the dispersion of the distribution, can be used to obtain further information about the dynamics of the system. Kazakov and Frenklach (1998), Kazakov et al. (1995) and Yoshihara et al. (1994) recently extended this numerical method and the corresponding model for soot formation.

Sectional techniques have been developed by Gelbard and Seinfeld (1978, 1980) and are presently used by Smooke et al. (1999) to derive information about soot particle size distributions. These methods are limited by the number of sections, which can be treated within acceptable computing times. From these calculations, the global values  $N$  and  $F_V$  can be obtained, however, the detailed structure of the size distribution of PAHs and soot particles remains in many applications unresolved.

In Appel et al. (1999), a detailed chemical model for soot formation was treated with a discrete h-p-Galerkin method (Wulkow, 1996). It has been shown that the method can be used to calculate size distributions of soot particles and PAH molecules and that the profiles of soot volume fraction and particle number density are quantitatively comparable to the results from the method of moments.

The present work is focused on the additional information, which can be obtained from the size distributions. For this, the impact of the single submodels on the dynamics of the PAH and soot particle ensemble is demonstrated.

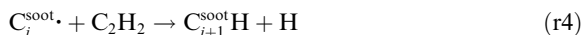
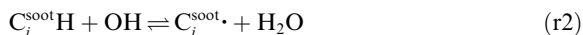
Especially, the particle inception submodel is studied in detail. An estimation of the size of the PAHs, which collide to form three-dimensional structures is presented. For this, MP2 quantum chemical calculations were performed to evaluate the interaction energy of PAH dimers.

## 2. Model of soot formation and oxidation

The model of soot formation and oxidation, which is used in the present work is equivalent to the one given in Appel et al. (2000). Therein, a detailed study of laminar premixed flames of  $C_2$  hydrocarbons was performed. The gas phase mechanism describes the pyrolysis and oxidation of the fuel molecules and the main combustion

reactions, which form carbondioxide and water. This part of the mechanism is based on the GRI-Mech1.2 (Frenklach et al., 1995) and its improvements in Appel et al. (2000) by the implementation of a new vinyl oxidation submechanism (Mebel et al., 1996). The formation and growth of linear aliphatic and polycyclic aromatic hydrocarbons are described with the mechanism by Wang and Frenklach (1997), which was extended by a new class of growth reactions (Appel et al., 2000). This reaction class includes all those acetylene addition processes, which show an intermediate H-radical migration as described in Frenklach et al. (1999). The PAH chemistry is described by a detailed chemical mechanism up to pyrene, whereas the further growth of the aromatic molecules is assumed to follow the hydrogen abstraction and carbon addition (HACA) reaction sequence (Frenklach, 1985). The particle inception step is modeled through the coalescence of PAHs. The dynamics of the solid soot phase includes coagulation, PAH addition to the soot surface as well as heterogeneous surface reactions. The reactions of gas phase species with the soot surface determine – depending on the surrounding gas mixture and temperature – the rate of growth or shrinkage of the particles. The particles are oxidized by OH-radicals and molecular oxygen, whereas they grow by the addition of acetylene, which is identified in different work (see Bockhorn, 1994 and references therein) to be the main growth species in laminar premixed flames. The size distribution of the soot particles, therefore, is discretized by the mass of two carbon atoms.

The mechanism for the heterogeneous surface reactions reads as follows:



We consider chemical recoupling due to heterogeneous reactions. In general, the consumption of chemical species by reactions with the soot surface has a minor impact on flames with low soot concentration. However, for completeness, these effects are considered in the present work. A model of aggregation as introduced by Kazakov and Frenklach (1998) has been omitted because TEM measurements (Bockhorn et al., 1986) of

soot particles in the studied flame show exclusively spherical particles under the prevailing conditions.

### 3. Mathematical formulation of the model

The prediction of soot formation and oxidation with the above-described kinetic model requires knowledge of the concentrations of the relevant chemical species and the flame temperature. Therefore, the conservation equations for the energy and mass fractions of the corresponding chemical species are solved. In one-dimensional geometry and steady-state flames, these equations are as follows:

$$\rho v c_p \frac{dT}{dy} = \frac{d}{dy} \left( \lambda \frac{dT}{dy} \right) - \frac{dT}{dy} \sum_{i=1}^{n_s} c_{pi} \rho Y_i v_i - \sum_{i=1}^{n_s} h_i w_i - q_r, \quad (1)$$

$$\rho v \frac{dY_i}{dy} = - \frac{d}{dy} (\rho Y_i v_i) + w_i W_i \quad (i = 1, \dots, n_s). \quad (2)$$

In the above equations,  $Y_i$  is the mass fraction of the species  $i$ .  $v_i$  identifies the diffusion velocities and  $w_i$  the chemical production and consumption rates of the species  $i$  with the molar masses  $W_i$ .  $c_{pi}$  is the heat capacity of the species  $i$  and  $h_i$  its molar enthalpy. The chemical rate terms also include the rates of formation and destruction of chemical species due to heterogeneous reactions with the soot surface. The rate of acetylene consumption by surface growth of soot can be expressed as follows:

$$w_{C_2H_2} = -\alpha k_{r4} [C_2H_2] \cdot \chi_{C^{soot}} \cdot \frac{W_{C_2H_2}}{N_A} \cdot S. \quad (3)$$

In Eq. (3),  $\chi_{C^{soot}}$  is the fraction of radical sites on the surface of the soot particles.  $\alpha$  is the fraction of the surface area  $S$ , which is available for chemical reactions (Appel et al., 2000; Frenklach and Wang, 1991).  $N_A$  means the Avogadro-number.

The term  $q_r$  considers the heat loss due to radiation of soot particles. It is modeled by using the temperature variation of the radiation coefficient of soot which gives the simple expression

$$q_r = CF_V T^5, \quad (4)$$

where  $C$  is a constant and  $F_V$  represents the soot volume fraction. The solution of Eqs. (1) and (2) for a number of chemical species prescribed by the adopted chemical mechanism (Frenklach et al., 1995; Mebel et al., 1996) forms the framework for the simulation of the dynamics of the PAH and the soot particle ensemble.

The surface growth mechanism considers acetylene to be the main growth species. Therefore, the size distribution of the soot particles is discretized by the mass of two carbon atoms. From this, a set of balance equations

for the soot particle number densities of the different particle sizes can be derived

$$\rho v \frac{d(N_i/\rho)}{dy} = \frac{d}{dy} \left( \rho D_i \frac{d(N_i/\rho)}{dy} \right) + \frac{d}{dy} \left( 0.55 v \frac{1}{T} \frac{dT}{dy} N_i \right) + S(N_i). \quad (5)$$

In Eq. (5), the second term on the right-hand side describes the transport of soot particles due to thermophoresis. In laminar premixed flames, the region of steep gradients in temperature exhibits low soot particle number densities, so that the effect of thermophoresis on the soot particle ensemble is small. The diffusion coefficient of soot particles in the single size classes is denoted by  $D_i$ . Seinfeld (1986) showed that the diffusion coefficient of an aerosol of very small particles is proportional to  $d^{-2}$ , where  $d$  is the diameter of the particles. The term  $S(N_i)$  represents the source of particles  $N_i$  in the size class  $i$  from all underlying chemical and physical processes of the model for soot formation.

As stated before, the smallest difference between two soot particles is the mass of two carbon atoms. Soot particles can consist of about  $10^7$  carbon atoms and, therefore, the number of balance equations would be of the same order of magnitude.

An efficient way of deriving information from this set of differential equations was introduced by Frenklach and Harris (1987). The definition of the statistical moments of the particle size distribution (PSDF)

$$M_r = \sum_{i=1}^{\infty} i^r N_i \quad (6)$$

leads to a new set of balance equations for the moments of the size distribution

$$\rho v \frac{d(M_r^{soot}/\rho)}{dy} = \frac{d}{dy} \left( \rho D_1 \frac{d(M_{(r-2)/3}^{soot}/\rho)}{dy} \right) + \frac{d}{dy} \left( 0.55 v \frac{1}{T} \frac{dT}{dy} M_r^{soot} \right) + S(M_r^{soot}). \quad (7)$$

The solution of equations for a set of moments of the PSDF was performed with SOFOKLES, an in-house program package, which is based on CHEMKIN II (Kee et al., 1980). The PAH growth was modeled with a technique introduced by Mauss et al. (1994) with the rate coefficients given by Kazakov et al. (1995).

The method of moments is a strong numerical tool for the computation of particle number densities and soot volume fractions. However, the full information about the soot particle and the PAH size distributions are not provided, and the impact of different models or the underlying physics on the PSDF is hard to quantify. From the numerical point of view, furthermore, the method of

moments has the disadvantage that a closed formulation of the equations of the moments is often not possible. These problems are solved, e.g. by a logarithmic Lagrangian interpolation (see Frenklach and Harris, 1987).

From these considerations, a numerical method, which supplies the full particle size distribution in high resolution is a necessary component for the modeling of soot formation. A high resolution is the major computational problem of the sectional method of Gelbard and Seinfeld (1978). Wulkow (1996) formulated a discrete h-p-Galerkin method for polymerization reactions. It is a powerful algorithm for the calculation of different distributions up to any polymer degree or particle size. For modeling of soot formation the algorithm allows the solution of the system of differential equations describing the dynamics of particles of specific sizes in a Lagrangian coordinate.

$$\frac{dN_i}{dt} = f(N_1, N_2, \dots, N_m), \quad i = 1, 2, \dots, m. \quad (8)$$

In Eq. (8),  $N_i$  is the number density of particles, which are built up from  $i$  monomer units. The algorithm approximates the size distributions by a multilevel Galerkin h-p-method with a work-oriented refinement strategy. The particle size axis is subdivided into several intervals and on each of these intervals an expansion  $N_i^j$  approximates the size distribution function of  $\mathbf{N}$ .

$$N_i^j|_{I_l} = \sum_{k=0}^{p_l^j} a_{ki} t_{ki}(i). \quad (9)$$

In Eq. (9),  $j$  is the number of the level and  $l$  the number of the interval. The polynomials  $t_{ki}(i)$  are discrete Chebyshev polynomials of the degree  $k$ . The number of expansion coefficients  $p_l^j$  may differ from interval to interval such that the size distribution can be resolved by varying grid and order.

A crucial feature of this type of approximation is that the number of degrees of freedom is low. This is particularly important in the presence of the coagulation operator, because the evaluation of a convolution sum with an arbitrary kernel function is very costly.

Coagulation is described by the Smoluchowski equation (Smoluchowski, 1917)

$$\frac{dN_i}{dt} = \frac{1}{2} \sum_{j=1}^{i-j} \beta_{j,i-j} N_j N_{i-j} - \sum_{i=1}^{\infty} \beta_{i,j} N_i N_j. \quad (10)$$

Here,  $\beta_{i,j}$  is the size-dependent frequency factor, which can be determined from the formula of Brownian motion

$$\beta_{i,j} = 2.2 \left( \frac{3m_1}{4\pi\rho_s} \right)^{1/6} \left( \frac{6k_b T}{\rho_s} \right)^{1/2} \cdot \sqrt{\frac{1}{i} + \frac{1}{j}} \cdot (i^{1/3} + j^{1/3})^2. \quad (11)$$

The mass density of soot is assumed to be  $\rho_s = 1.8 \text{ g/cm}^3$  (Frenklach and Wang, 1991) and  $m_1$  indicates the mass of a monomer unit, which is a  $C_2$ -group.

The h-p-discretization of the size classes is combined with a time discretization by means of the Rothe method (Rothe, 1930). This technique was introduced by Bornemann (1991) for parabolic differential equations and was transferred and extended to polyreaction kinetics in Wulkow (1996).

For an approximation  $\mathbf{N}^1$  of the solution  $\mathbf{N}(t + \tau)$  after a time step from  $t$  to  $t + \tau$ , we apply the semi-linear-implicit Euler scheme

$$\begin{aligned} (\mathbf{I} - \tau\mathbf{A})\Delta\mathbf{N} &= \tau f(\varphi), \\ \mathbf{N}^1 &= \varphi + \Delta\mathbf{N} \end{aligned} \quad (12)$$

and the correction step

$$\begin{aligned} (\mathbf{I} - \tau\mathbf{A})\eta^1 &= -\frac{1}{2}\tau^2\mathbf{A}f(\varphi), \\ \mathbf{N}^2 &= \mathbf{N}^1 + \eta^1, \end{aligned} \quad (13)$$

such that no additional linear system has to be treated (Deuffhard, 1985). In the above equations, the vector  $\mathbf{N}$  contains information about the PSDF, viz. the number densities  $N_i$  of the size class  $i$ ,  $\mathbf{I}$  is the identity matrix and the matrix  $\mathbf{A}$  contains the derivatives ( $dN_i/dN_j$ ), which describe the dynamics of the system.

#### 4. Studied flame

In this work, a laminar premixed flat acetylene/oxygen/argon flame with a C/O-ratio of 1.1 is the subject of investigation. The flow velocity of the cold gas is 20.1 cm/s. The feed contained 60 mol% of argon. The flame was stabilized at a pressure of 120 mbar. For this flame, a number of experimental data are available to validate the applied detailed model. Bockhorn et al. (1983) measured the concentration profiles of the main combustion species as well as those of linear aliphatic and polycyclic aromatic hydrocarbons. Bockhorn et al. (1983) and Wannemacher (1983) determined the flame temperature. The profiles of particle number density and soot volume fraction are also provided in Bockhorn et al. (1983). In addition to these data, soot particle size distributions were derived from the evaluation of TEM-microscopy pictures, which were recorded at different heights above the burner (Bockhorn et al., 1986; Heddich, 1986).

#### 5. Results and discussion

Before discussing the formation of PAH molecules, the main combustion process in the flame, including the

heat release of the flame, has to be addressed. A precondition for the modeling of PAHs is the correct prediction of major chemical species and temperature. Similarly, if the PAH concentrations are predicted in the correct order of magnitude, the physical and chemical processes leading to soot particle formation and growth can be addressed. If the total particle number density and soot volume fraction match with the experimental observations, then the evolution of the soot particle size distribution can be examined.

### 5.1. Gas phase chemistry

The gas phase mechanism has been adopted unchanged from the model presented in Appel et al. (2000). In Fig. 1, the experimental profiles of the mole fractions of different major gas phase species (Bockhorn et al., 1983) are compared with the calculated values. With the exception of the mole fraction of  $\text{CO}_2$ , the agreement between simulation and experiment is excellent.  $\text{CO}_2$  is overpredicted by about 20%. The calculated temperature fits the measured ones as well. It can be seen in Fig. 1 that the flame temperature decreases with higher heights above the burner. In the simulation, this effect is attained by modeling the radiation as given in Eq. (4).

In Fig. 2, the experimentally determined mole fractions of higher linear hydrocarbons, benzene, and naphthalene, are depicted in comparison with the results from numerical simulation. The agreement is acceptable, though generally a shift of the computed mole fraction profiles to the left can be observed. The reason for this may be the distortion of the flame by the sampling probe in the experiments.

The quality of description of the chemical reactions in the gas phase is crucial for the simulation of soot formation, because heterogeneous surface growth reactions, which are dependent on the hydrogen atom or

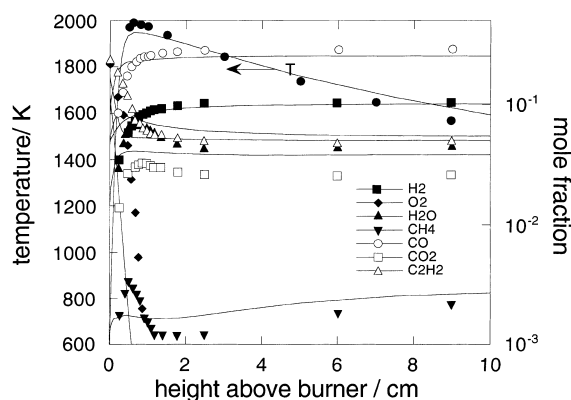


Fig. 1. Comparison of calculated and measured profiles of flame temperature and mole fractions of major combustion species.

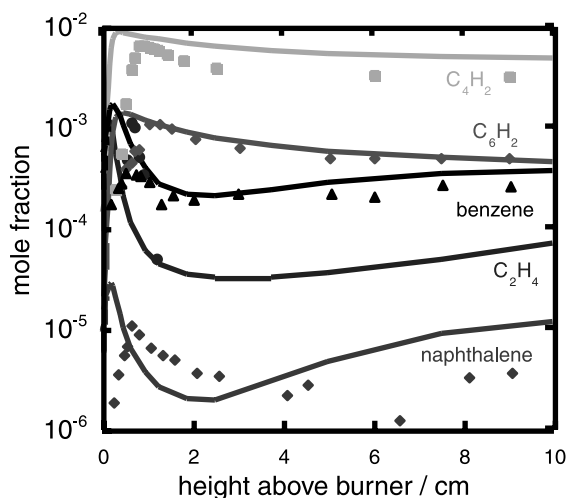


Fig. 2. Comparison of calculated and measured profiles of mole fractions of larger linear aliphatic and aromatic hydrocarbons.

OH-radical concentrations, are the most important sources of soot mass in low pressure premixed flames. The results given in Figs. 1 and 2 demonstrate that the model for the gas phase reactions gives a good description of the structure of the studied flame. This enables the study of PAH growth and soot particle dynamics.

### 5.2. Large PAH chemistry and soot formation

In this work, the method of moments and a discrete h-p-Galerkin method have been used to calculate the profiles of particle number densities and soot volume fractions in the flame. In the case of the latter method, these quantities are determined from the particle size distribution. The particle number density is dependent on the definition of a particle. In the present model, a particle is a three-dimensional cluster of PAH structures, which is formed by PAH coalescence. The pyrene molecule is supposed to be the smallest aromatic component, which forms three-dimensional dimers. A justification of this assumption is given in the following section. By this assumption, PAH molecules consisting of more carbon atoms are still treated as gas phase species. When comparing soot particle number densities from simulation and experiment the definition of particles in the solid phase and gas phase species has to be kept in mind.

#### 5.2.1. PAH size distribution and particle inception

The PAH chemistry is treated with a detailed reaction mechanism (Appel et al., 2000; Frenklach et al., 1995; Mebel et al., 1996; Frenklach et al., 1999) for PAHs up to pyrene. The growth of aromatic molecules

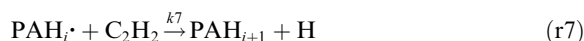
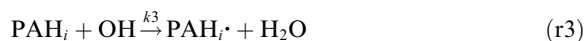
beyond pyrene is described by the hydrogen abstraction carbon addition reaction sequence (Frenklach, 1985) assuming quasi-steady-state assumptions. The sequence of hydrogen abstraction and carbon addition has been supposed to be a good approximation for the major growth steps. In order to save computing time during the application of the h-p-Galerkin method only condensed PAHs and those molecules, which have a radical site at the edge of the molecule have been considered. The detailed structure of the aromatic species is not included. Note that this is not a restriction of the mathematical method in general. From these assumptions, the mathematical representations of the PAHs are two different size distributions; one for the radical species, the second for the condensed molecules. PAH species with two radical sites have not been considered.

The reactions, which are involved in PAH formation, growth, and oxidation are as follows:

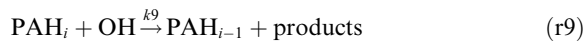
#### PAH formation



#### PAH growth



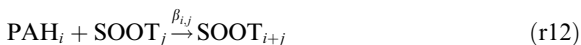
#### PAH oxidation



#### Particle inception



#### PAH addition



As pyrene (pyrene consists of eight monomer units: PAH<sub>8</sub>) is assumed to be the smallest molecule, which is involved in particle inception and surface growth due to PAH addition, species smaller than pyrene that are formed by oxidation are removed from the distribution. Reactions (r10–r12) are mathematically equivalent to coagulation. Particle inception due to coalescence of two radical PAH molecules is neglected in the model. This can be justified by the low concentration of the radical aromatic species in comparison to the stable PAHs. In general, the concentration of radical PAHs is by more than a factor of one fifth lower than the one of the corresponding PAHs. Hence, the particle formation rate from two radical PAHs is by more than a factor of 1/25 lower than the rate of reaction (r10).

In the following, the effect of particle inception and PAH addition to the surface on the evolution of the PAH size distribution is demonstrated. For this purpose, three simulation runs have been performed. In run 1, only PAH growth and oxidation were considered. Particle inception and PAH addition to soot were not included. The second run included PAH growth and oxidation as well as particle inception and in run 3, the full model, including PAH addition to soot, was used. In Fig. 3, the evolution of the PAH size distributions in the three test runs is depicted. In run 1 (Fig. 3(a)), large PAH molecules are formed due to the growth reactions. After a few milliseconds, the oxidation reactions no longer compete with the PAH growth reactions because the concentration of molecular oxygen and hydrogen radicals are low. Towards longer reaction time the total number of PAHs increases permanently. Run 2 (Fig. 3(b)) exhibits a totally different behavior of the PAH size distribution. Owing to soot particle formation, the PAHs are removed from the distribution. This effect increases with increasing PAH concentrations. After 12 ms particle formation competes with the initiation reaction (r1). The maximum PAH number density is about one order of magnitude lower as compared with run 1. In the main reaction zone (reaction time 10–16 ms), larger PAHs with up to 20 carbon atoms are formed. After the decay of the growth rates the initiation step again dominates the shape of the PAH distribution, so that the maximum of the distribution is again with sizes in the order of magnitude of 16–18 carbon atoms. The effect of PAH consumption due to a transition into the solid soot phase is more pronounced when the PAH surface addition is taken into account. In run 3 (Fig. 3(c)), all the submodels are considered. The rate of PAH soot-collisions is dependent on the number density and the size of the soot particles in the flame. Therefore,

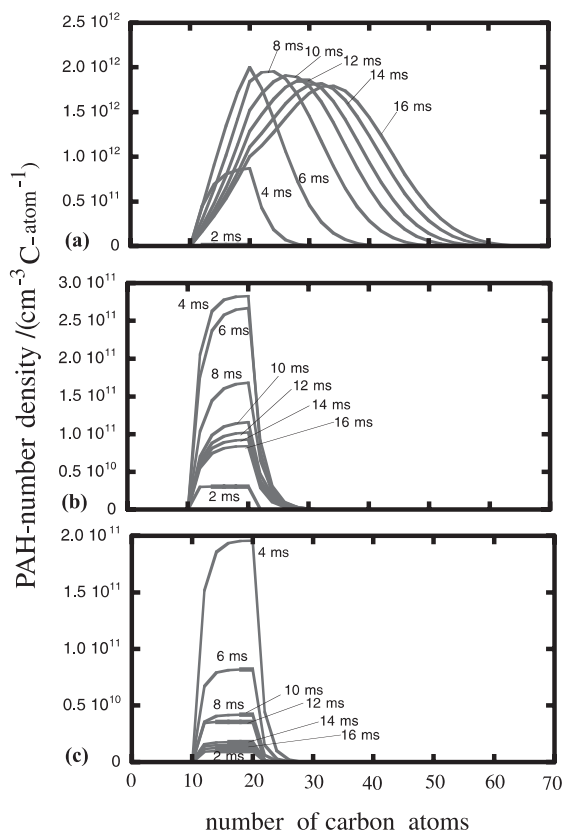


Fig. 3. Calculated PAH size distributions with different model assumptions, for further explanation, see text.

the PAH distribution is rather narrow during the entire reaction time for this case.

From these simulations, the influence of the single processes, viz. PAH formation, PAH growth, particle inception, and PAH addition to the soot surface on the evolution of the PAH size distribution is obvious. Particle inception and PAH formation seem to have the largest impact on the PAH dynamics, whereas the growth of the PAHs is relatively insignificant in the investigated flame. The addition of PAHs to the soot surface is more important for the shape of the soot particle size distribution because it competes with particle inception. This will be discussed in the following section after examining the particle inception submodel in more detail.

Bockhorn et al. (1983) and Wenz (1983) determined the concentration profiles of a number of aromatic species in the flame under consideration. They used molecular beam sampling and collected sufficient material to perform analysis by coupled gas chromatography/mass spectrometry. The limit of reliable detection of the method was in the size range of coronene (C<sub>24</sub>). In Fig. 4(a), comparison between the simulated PAH size distribution at 12 ms and the corresponding PAH con-

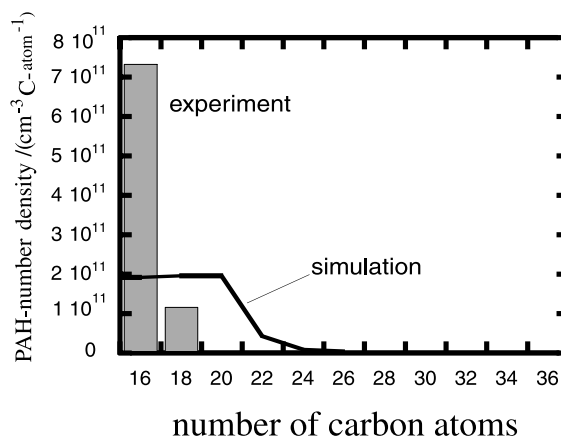


Fig. 4. Comparison of the experimentally determined PAH size distribution with the result of the calculated ones. The distributions were taken at a reaction time of 12 ms, which corresponds to the maximum PAH concentration.

centrations from the experiment for PAHs larger than pyrene are depicted. Simulation and experiment show qualitative agreement. In the experiment, aromatic compounds larger than C<sub>18</sub> could be found only in concentrations not appearing in the scale of Fig. 4.

In Fig. 5, the profiles of the total soot particle number density and the soot volume fraction are shown. It can be seen that the particle inception model is capable of reproducing the number of particles in the studied flame. It is also demonstrated that both the mathematical methods generate quantitatively comparable results.

From the results in Figs. 3–5, we conclude that soot particles are formed from the coalescence of PAH

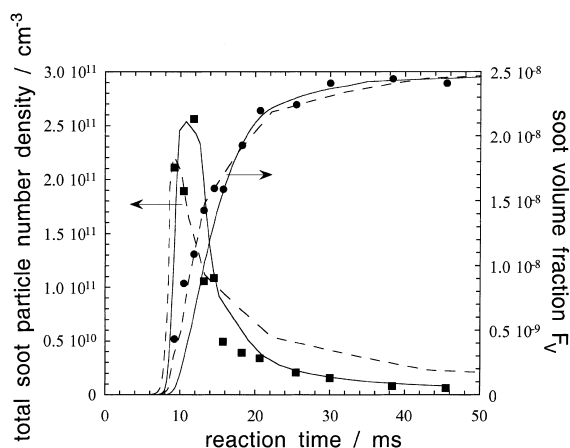


Fig. 5. Comparison of the experimental data for the total particle number densities and the soot volume fractions. The dashed lines represent results from the method of moments. The solid lines are derived from the evolution of the particle size distribution calculated with the discrete h-p-Galerkin method.

molecules with 16–20 carbon atoms. Therefore, the interaction energy of PAHs of this size must be sufficiently large to make the molecules stick together and form three-dimensional structures. The number density of larger aromatic species is too low to generate particle inception rates as measured in the studied flame. If PAH molecules of this size were not responsible for particle inception, larger aromatic species should be found in the flame in considerable higher concentrations (see Fig. 3).

To validate this hypothesis, the interaction energy between two PAH molecules during collision has been estimated using MP2 (Möller–Plesset second-order perturbation correction to the SCF energy) level calculations. The interaction energy is the energy of formation of a layered dimer of eclipsed geometry from two single PAH molecules. The interaction energy per carbon atom of 6 kJ/mol, which was determined by Stein et al. (1977), is a first approximation of the expected values. The calculations have been performed with the *TURBO-MOLE*-code (Ahlrichs et al., 1989; Schäfer et al., 1992; Haase and Ahlrichs, 1993; Stone, 1996; Weigand and Häser, 1997; Weigand et al., 1998) employing several steps of refinement of the basis sets. These refinement steps reduced the basis set superposition error to about 13.17% of the binding energy (benzene dimer).

Generally, the dimers should be stable under flame conditions, if the interaction energy in the dimer is larger than the internal energy of the two molecules. The internal energy should be equally distributed among the translational and rotational degrees of freedom. The excitation of vibrational degrees of freedom is strongly dependent on temperature. Therefore, as the lowest limit estimate, the contribution of the vibrational modes was neglected. The six degrees of freedom from translation and rotation result in an energy per mole of 6 RT so that the interaction energy in the PAH dimer should be larger than 6 RT to form a stable structure.

A conformation of the dimers comparable to the graphite structure, where the C-atoms in one layer are in the center of the C<sub>6</sub> rings of the neighboring layers, increased the computing time for large polycyclic aromatic structures drastically. Therefore, in order to save computing time, the conformation of the dimers has been chosen to be eclipsed (symmetry D<sub>2h</sub>). This geometry results in lower interaction energies compared with the graphite structure. On the other hand, the computed 0 K interaction energies are the highest possible values for a given geometry, so that the calculations are on the order of magnitude calculations.

The interaction energy in the benzene dimer was calculated to be 15.5 kJ/mol. In the naphthalene, anthracene, and pyrene dimers, the energies are 30.9, 54.6 and 73.8 kJ/mol, respectively. In Fig. 6, the results of the calculations for the 0 K interaction energy of the studied dimers are plotted together against the estimate of the internal energies of the PAHs (6RT). It can be seen that

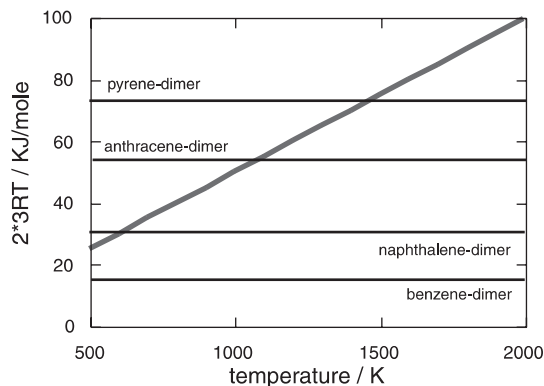


Fig. 6. Estimated internal energies of the aromatic molecules at different temperatures. The horizontal lines indicate the 0 K interaction energies of four different dimers from MP2 calculations.

the calculated interaction energies for PAH dimers larger than the pyrene dimer is sufficiently high to form a stable three-dimensional structure at temperatures above 1500 K. Smaller aromatic molecules obviously are not able to form stable layered structures in the studied flame.

The information obtained from the present ab initio calculations confirm the idea, that soot particles grow from three-dimensional layered oligomers that are formed by PAH collisions. Under sooting conditions, these processes occur at higher rates than the planar growth of PAHs and the formation of planar oligomers, that have been observed in pyrolyses (Mukherjee et al., 1994). Also the assumption that pyrene is the smallest aromatic molecule, which is responsible for particle formation appears to be reasonable.

#### 5.2.2. Soot particle size distributions

Before discussing the results of the complete model, we focus on PAH addition to the soot surface and on particle coagulation. In Fig. 7, the size distributions of the soot particles are presented for a run where solely particle inception and PAH addition are included. In the previous section, very narrow PAH size distributions have been found, when particle inception and PAH addition to the soot surface are taken into account. A consequence of this fact is that mainly PAHs of a specific number of carbon atoms collide with soot particles or PAHs. This results in a particle size distribution with maxima at particle sizes corresponding to integer multiples of the number of carbon atoms of the PAH molecules with the highest number density. As the particle diameter is not linearly dependent on the number of carbon atoms, the distance between the maxima along the particle diameter axis decays for larger particles.

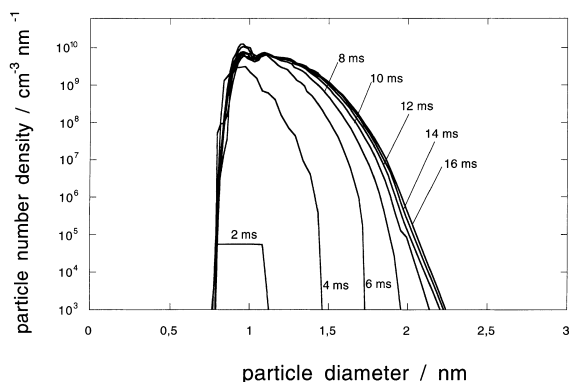


Fig. 7. Evolution of the soot particle size distributions for only particle inception and PAH addition to the soot surface being considered.

A similar effect can be observed, when solely particle inception and coagulation are solely considered. The evolution of the soot particle size distributions for this run is presented in Fig. 8. Here, the difference between the maxima corresponds to the size of the smallest particles. It can also be seen that coagulation has a much stronger influence on the PSDF than PAH addition to the surface. After 16 ms, particles with a diameter of up to 5 nm are formed, whereas in the case of pure addition of PAHs to the soot surface (Fig. 7) the particles are smaller than 2.5 nm.

When, in addition to PAH addition and particle coagulation, the heterogeneous surface reactions are included, the principle shapes of the soot particle size distributions remain similar to that in Fig. 8. Particle inception and coagulation still dominate the particle dynamics of the system. Surface growth affects the distribution in the main reaction zone. In this region, the main amount of soot is added to the solid phase by heterogeneous surface reactions with acetylene. The

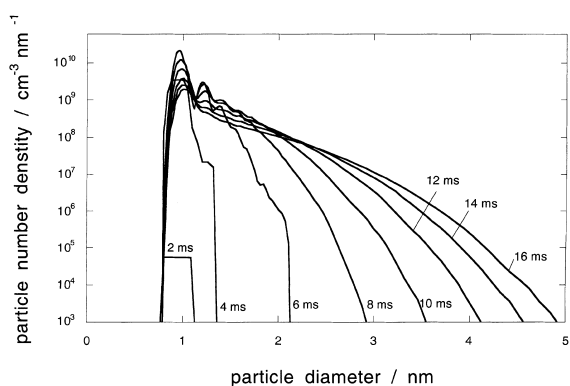


Fig. 8. Evolution of the soot particle size distributions for only particle inception and coagulation being considered.

width of the distribution increases rapidly during this process, compare Fig. 9. After the narrow surface growth zone, coagulation is the dominant source for the evolution of the PSDF.

The rate of surface growth is proportional to a fraction of the surface area of the soot particles, see Eq. (3). The particles are assumed to be spherical so that the surface area of a particle can be determined by

$$S_i = 4\pi \left( \frac{3m_i}{4\pi\rho_{\text{soot}}} \right)^{2/3} i^{2/3} \quad (14)$$

and the diameter of the particles is given by

$$d_i = 2 \left( \frac{3m_i}{4\pi\rho_{\text{soot}}} \right)^{1/3} i^{1/3}. \quad (15)$$

The two major processes in soot particle dynamics, viz. coagulation and surface growth, have a strong size dependence. For coagulation, high coagulation rates are obtained for the collisions of small particles with large ones due to the size dependence of the mean velocity of the particles and the collisional cross-sections. This causes a fast consumption of small particles. The size dependence of the rates of surface growth reactions implicates that the rate of acetylene addition is high for large particles. However, due to the size dependence of the ratio of surface area to diameter, in regions with many small particles, the relative surface area is high and so the overall soot growth rate is also large.

In Fig. 9, the evolution of the soot particle size distributions from a run with the complete model is presented. The surface growth reactions mainly affect the size distributions between 6 and 12 ms.

Finally, in Fig. 10, a comparison of the computed particle size distributions with experimentally determined distributions (Heddrich, 1986; Bockhorn et al., 1986, 1988) is presented. The experimental results are obtained from molecular beam sampling of the soot

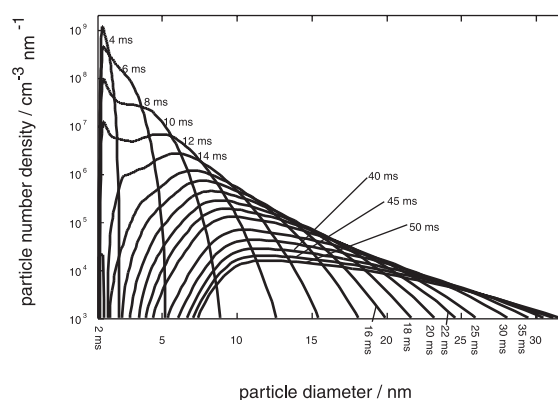


Fig. 9. Evolution of the soot particle size distributions from the simulation with the complete model.

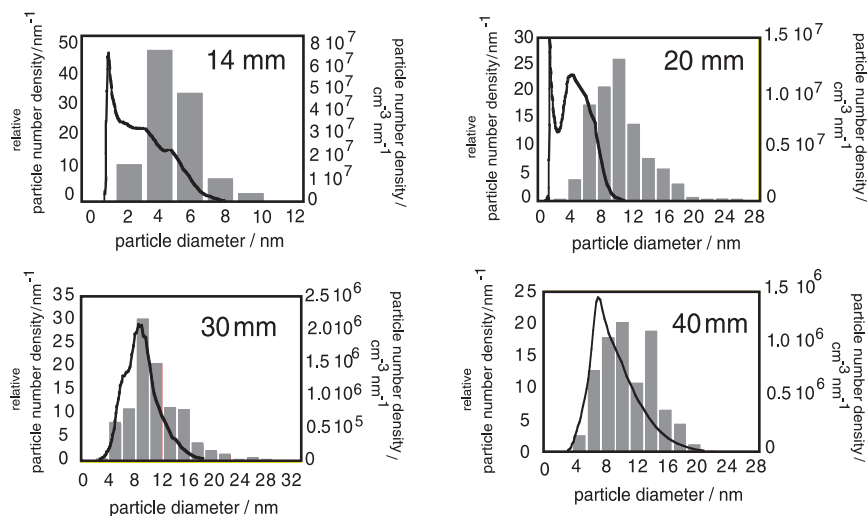


Fig. 10. Comparison of experimental and calculated soot particle size distributions. The relative number of particles in the experiment is the number of particles of a certain size divided by the total number of examined particles. Due to the experimental technique used in Heddrich (1986), Bockhorn et al. (1986), Bockhorn et al. (1988), a comparison of absolute numbers is not possible.

flame and TEM micrographs of the soot particles. The experimental values are relative particle number densities, which indicate the percentage of particles, which were found within a certain range of diameters. The lower detection limit of the experiments was reported to be about 1 nm. At low heights above the burner, the calculated soot particle size distributions show smaller particles than in the experimental observations. This can be explained by experimental uncertainties, because of the difficulty to extract the particles from the main reaction zone of the flame. It can also be a consequence of the definition of the difference between particles and gas phase PAH species. The agreement between the simulated and measured size distributions at 30 and 40 mm height above the burner is excellent.

## 6. Conclusion

In this work, a detailed numerical study of soot formation in a laminar premixed flame of acetylene was performed.

For this, two numerical methods, the method of moments and a discrete h-p-Galerkin method, were used to obtain information from the solution of the balance equations for the number densities of the soot particles and the PAH size classes. It could be shown, that both the numerical methods give quantitatively the same results for the total particle number densities and the soot volume fractions in the flame.

The examination of the PAH size distribution showed that particle inception by PAH coalescence is a reasonable assumption. Neglecting the addition of

PAHs to the solid soot phase leads to PAH sizes, which were not observed in the experiments. A second justification for the PAH coalescence inception model was given by a comparison of the interaction energies of PAH dimers with the internal energies of the molecules under flame conditions.

The dynamics of the soot particle ensemble are generally dominated by coagulation. Only in the main reaction zone the simultaneously ongoing surface growth influences the shape of the distribution. On the other hand, the total soot mass is strongly affected by surface growth reactions.

With the discrete h-p-Galerkin method, a new numerical method for soot formation modeling was introduced, which can be used for the simulation of soot formation in flames. A typical simulation run including the total particle dynamics model takes about 5–10 min on a Pentium II 350 MHz processor. The potential of the method is to provide more detailed information about the evolution of soot particle size distributions in flames.

## Acknowledgements

The ab initio calculations were performed by Klaus May and Dr. Stefan Dapprich, Institute of Physical Chemistry, University of Karlsruhe, within Sonderforschungsbereich 551 at the University of Karlsruhe. The help of Klaus May and Dr. Stefan Dapprich is acknowledged gratefully. Financial support from the Deutsche Forschungsgemeinschaft and the Bayerische Forschungsförderung is gratefully acknowledged.

**References**

- Ahlich, R., Bär, M., Häser, M., Horn, H., Kölmel, C., 1989. *Chem. Phys. Lett.* 162, 165.
- Appel, J., Bockhorn, H., Frenklach, M., 2000. Kinetic modeling of soot formation with detailed chemistry and physics. *Laminar premixed flames of C<sub>2</sub> hydrocarbons*, *Combust. Flame* 121, 122.
- Appel, J., Bockhorn, H., Wulkow, M., 1999. In: Keil, E., Mackens, W., Voß, H., Werther, J. (Eds.), *Scientific Computing in Chemical Engineering II*. Springer, Berlin, p. 94.
- Bockhorn, H. (Ed.), 1994. *Soot Formation in Combustion: Mechanisms and Models*. Springer, Berlin.
- Bockhorn, H., Fetting, F., Heddrich, A., 1986. 21st Symposium (International) on Combustion. The Combustion Institute, Pittsburgh, p. 1001.
- Bockhorn, H., Fetting, F., Wenz, H.W., 1983. *Ber. Bunsenges. Phys. Chem.* 87, 1067.
- Bockhorn, H., Fetting, F., Heddrich, A., Meyer, U., Wannemacher, G., 1988. *J. Aerosol Sci.* 19, 591.
- Bockhorn, H., Fetting, F., Wannemacher, G., Wenz, H.-W., 1983. 20th Symposium (International) on Combustion. The Combustion Institute, Pittsburgh, p. 1423.
- Bornemann, F.A., 1991. *Impact Comput. Sci. Eng.* 3, 93.
- Deuffhard, P., 1985. *SIAM-Rev.* 27 (4).
- Frenklach, M., 1985. *Chem. Eng. Sci.* 40 (10), S1843.
- Frenklach, M., Harris, S.J., 1987. *J. Colloid Interface Sci.* 118, 252.
- Frenklach, M., Moriarty, N.W., Brown, N.J., 1999. 27th Symposium (International) on Combustion. The Combustion Institute, Pittsburgh, p. 1655.
- Frenklach, M., Wang, H., 1991. 25th Symposium (International) on Combustion. The Combustion Institute, Pittsburgh, p. 1559.
- Frenklach, M., Wang, H., Goldenberg, M., Smith, G.P., Golden, D.M., Bowman, C.T., Hanson, R.K., Gardiner, W.C., Lissianski, V., 1995. GRI Technical Report No. GRI 95/0058, Gas Research Institute.
- Gelbard, F., Seinfeld, J.H., 1978. *J. Comput. Phys.* 28, 357.
- Gelbard, F., Seinfeld, H.J., 1980. *J. Colloid Interface Sci.* 485, 78.
- Haase, T., Ahlich, R., 1993. *J. Comput. Chem.* 14, 907.
- Heddrich, A., 1986. Dissertation, Technische Hochschule Darmstadt.
- Kazakov, A., Frenklach, M., 1998. *Combust. Flame* 114, 484.
- Kazakov, A., Wang, H., Frenklach, M., 1995. *Combust. Flame* 100, 111.
- Kee, R.J., Miller, J.A., Jefferson, T.H., 1980. CHEMKIN: A general-purpose, problem-independent, transportable, fortran chemical kinetics code package, Sandia National Laboratories Report, SAND80-8003, Sandia National Laboratories.
- Kennedy, I.M., 1997. *Prog. Energy Combust. Sci.* 23, 95.
- Leung, K.M., Lindstedt, R.P., 1995. *Combust. Flame* 102, 129.
- Marinov, N., Pitz, W.J., Westbrook, C.K., Castaldi, M.J., Senkan, S.M., 1996. *Combust. Sci. Tech.* 116-117, 311.
- Mauss, F., Trilken, B., Breitbach, H., Peters, N., 1994. In: Bockhorn, H. (Ed.), *Soot Formation in Combustion: Mechanisms and Models*. Springer, Berlin, p. 325.
- Mebel, A.M., Diau, E.W.E., Lin, M.C., Morokuma, K., 1996. *J. Am. Chem. Soc.* 118, 9759.
- Mukherjee, J., Sarofim, A.F., Longwell, J.P., 1994. *Combust. Flame* 96, 191.
- Rothe, E., 1930. *Math. Ann.* 102, 650.
- Schäfer, A., Horn, H., Ahlich, R., 1992. *J. Chem. Phys.* 97, 2571.
- Seinfeld, J.H. (Ed.), 1986. *Atmospheric Chemistry and Physics of Air Pollution*. Wiley, New York, pp. 324.
- Smoluchowski, M.V., 1917. *Z. Phys. Chem.* 92, 129.
- Smooke, M.D., McEnally, C.S., Pfefferle, L.D., Hall, R.J., Colket, M.B., 1999. *Combust. Flame* 117, 117.
- Stein, S.E., Golden, D.M., Benson, S.W., 1977. *J. Phys. Chem.* 81, 314.
- Stone, A., 1996. *The Theory of Intermolecular Forces*. Clarendon Press, Oxford.
- Wang, H., Frenklach, M., 1997. *Combust. Flame* 110, 173.
- Wannemacher, G., 1983. Dissertation, Technische Hochschule Darmstadt.
- Weigand, F., Häser, M., 1997. *Theoret. Chem. Acc.* 331, 97.
- Weigand, F., Häser, M., Patzelt, H., Ahlich, R., 1998. *Chem. Phys. Lett.* 294, 143.
- Wenz, H.W., 1983. Dissertation, Technische Hochschule Darmstadt.
- Wulkow, M., 1996. *Macromol. Theory Simul.* 393, 5.
- Yoshihara, Y., Kazakov, A., Wang, H., Frenklach, M., 1994. 25th Symposium (International) on Combustion. The Combustion Institute, Pittsburgh, p. 941.